
Weighted Meta-Learning

Diana Cai

Princeton University
Princeton, NJ 08544
dcai@cs.princeton.edu

Rishit Sheth

Microsoft Research New England
Cambridge, MA 02142
rishet@microsoft.com

Lester Mackey

Microsoft Research New England
Cambridge, MA 02142
lmackey@microsoft.com

Nicolo Fusi

Microsoft Research New England
Cambridge, MA 02142
fusi@microsoft.com

Abstract

Meta-learning leverages related source tasks to learn an initialization that can be quickly fine-tuned to a target task with limited labeled examples. However, many popular meta-learning algorithms, such as model-agnostic meta-learning (MAML), only assume access to the target samples for fine-tuning. In this work, we provide a general framework for meta-learning based on weighting the loss of different source tasks, where the weights are allowed to depend on the target samples. In this general setting, we provide upper bounds on the distance of the weighted empirical risk of the source tasks and expected target risk in terms of an integral probability metric (IPM) and Rademacher complexity, which apply to a number of meta-learning settings including MAML and a weighted MAML variant. We then develop a learning algorithm based on minimizing the error bound with respect to an empirical IPM, including a weighted MAML algorithm, α -MAML. Finally, we demonstrate empirically on several regression problems that our weighted meta-learning algorithm is able to find better initializations than uniformly-weighted meta-learning algorithms, such as MAML.

1 Introduction

The applicability of machine learning techniques to real-world problems is often limited by the quantity of labeled data available. This is particularly detrimental when high-accuracy, high-capacity models are needed for a given application, since their requirements on the amount of data are particularly onerous. As a result, examples of these issues are wide-ranging and can be identified in vision (Koch, 2015), language modeling (Vinyals et al., 2016), content recommendation (Vartak et al., 2017), character generation (Lake et al., 2015), and health care (Zhang et al., 2019; Altae-Tran et al., 2017).

One crucial observation to overcome this challenge is that while data on the *target* task may be limited, other *source* tasks can be used to help with learning. This is precisely the setting considered in meta-learning, wherein multiple source tasks are used to provide a good “initialization” to learn on a target task. Some recent developments in meta-learning include metric-based methods (Lake et al., 2015; Koch, 2015; Vinyals et al., 2016; Snell et al., 2017; Oreshkin et al., 2018), model-based methods (Santoro et al., 2016; Munkhdalai and Yu, 2017), optimization-based methods (Ravi and Larochelle, 2016), and gradient-based methods (Finn et al., 2017; Nichol et al., 2018).

In gradient-based meta-learning, the goal is to learn an initialization from a set of source tasks that can be quickly adapted to a new target task with a small number of gradient steps. Within gradient-based

meta-learning methods, model-agnostic meta-learning (MAML) (Finn et al., 2017) is a popular approach that leverages data from a collection of source tasks to learn an initial model that can be quickly adapted to some target data task, often using a limited number of labeled target examples. A key feature of MAML is that it does not require a particular type of learning model or architecture and is therefore broadly applicable to problems in regression, classification, and reinforcement learning. A number of extensions to MAML (Nichol et al., 2018; Antoniou et al., 2018; Song et al., 2020) have since been proposed, and connections to hierarchical Bayesian modeling have been drawn (Grant et al., 2018; Yoon et al., 2018; Finn et al., 2018; Ravi and Beatoon, 2019; Jerfel et al., 2019).

An important assumption in many gradient-based meta-learning methods is that the source and target tasks are drawn from the same task distribution. Since the true task distribution is usually unknown, implicit in this assumption is that future target tasks will be uniformly similar to the source tasks. In practice, this assumption is encoded in the algorithm as uniformly sampling from the source tasks during meta-training (Finn et al., 2017; Nichol et al., 2018). However, a target task may be similar to only a few of the source tasks, or even just one, and applying equal weighting to all sources during meta-learning can be detrimental. Indeed, recent research in extending the MAML framework by modeling hierarchical task distributions (Yao et al., 2019), task non-stationarity (Nagabandi et al., 2018), and multi-modality (Vuorio et al., 2018) attempts to address this shortcoming with more complex meta-learners, and other meta-learning methods have noted the importance task similarity (Achille et al., 2019; Jomaa et al., 2019). Here, we instead note that in many practical applications, the target task is available during training, and focus on the goal of minimizing the loss of the specific target task during the *entire* training procedure, rather than just the adaptation step. Specifically, we propose using the labeled target task samples during meta-training to learn a better initialization for a given target task.

We study a general class of meta-learning methods that can be described by a task-weighted meta-objective; this general class captures a variety of gradient-based meta-learning objectives, such as joint training and MAML (and first-order variants), as well as weighted variants of joint training and MAML. We make no assumptions on the distribution of the source and target tasks. Our meta-objective is designed to encode similarity between the task distributions by upweighting sources that are more similar to the target task. The similarity between source and target task distributions is captured by an integral probability metric (IPM), which is used to compare the empirical distributions of the tasks.

For this class of weighted meta-learning objectives, we provide data-dependent error bounds on the expected target risk in terms of an empirical IPM and Rademacher complexity. The resulting generalization bound leads naturally to a learning algorithm incorporating weight optimization. We show that the IPM calculation can be bounded by selecting a kernel that generates a reproducing kernel Hilbert space (RKHS) ball containing the class of functions described by composing the model class with the loss function. We provide examples on how to construct such an RKHS ball for squared loss (regression) and hinge loss (binary classification) with linear basis function models, which apply to weighted MAML and weighted ERM. Importantly, this approach defines task similarity explicitly in terms of performance rather than a proxy measure, e.g., task embedding distances.

In what follows, we first review related work that has considered task similarity in meta-learning (Section 2). We then describe our general meta-learning setup (Section 3.1) and present data-dependent generalization bounds (Section 3.2). An algorithm for minimizing the weights of the meta-objective that is used to learn the initial model is described in Section 4. Finally, we empirically demonstrate that a weighted meta-learning objective can lead to improved initializations over uniformly-weighted meta-learning objectives, which include joint training and MAML as special cases. In particular, we conduct experiments in synthetic linear and sine regression problems, as well as a number of multi-dimensional basis regression problems on real data sets (Section 5).

2 Related work

A number of recent works have established guarantees for gradient-based meta-learning algorithms (Finn et al., 2019; Khodak et al., 2019a,b) developed from the perspective of online convex optimization. Further work has also established guarantees for non-convex loss functions (Fallah et al., 2019). In these frameworks, task similarity is either not considered, or is fundamentally defined as distance between model parameters in some metric space (Khodak et al., 2019a,b), whereas we define task

similarity via an IPM that directly captures induced performance differences. Li et al. (2017); Xu et al. (2019) incorporate the use of task-weighted loss functions within MAML meta-training. However, the weights are found heuristically with no guarantees and are not explicitly related to task similarity.

A separate line of work in domain adaptation studies the problem of combining multiple source tasks with target task data. Early bounds for classification were established by Ben-David et al. (2010) in terms of an \mathcal{H} -divergence. Zhang et al. (2013, 2012) extend these results by considering general loss functions and deriving bounds in terms of a population IPM (and subsequently study convergence in this setting). Separately, Mansour et al. (2009b) considered the mixture adaptation problem of combining the predictions of given source models and showed that a distribution-weighted combining rule will achieve performance close to the lowest performing source model assuming the target is a mixture of sources. The ensemble generative adversarial network of Adlam et al. (2019) utilizes a discrepancy distance (Mansour et al., 2009a; Cortes and Mohri, 2014) to compute task weights, but utilizes fixed models in the ensemble to generate data for a target task, whereas we learn task weights to optimize a model for a target task directly. Similar to our setting, Pentina et al. (2019) also develop a data-dependent bound for meta-learning with weighted tasks; their bound, however, contains interaction terms between task weights and unobservable quantities (the minimum possible combined source/target error of a single hypothesis) which, unlike this work, precludes optimization with respect to task weights.

In a similar spirit to our work, Shui et al. (2019) consider the \mathcal{H} -divergence and Wasserstein distance as task similarity measures to develop generalization bounds in the setting of multi-task learning with finite VC- and pseudo-dimension model classes. In our construction, we embed the model class composed with loss function within a RKHS, allowing the task similarity measure to be efficiently computed by kernel distance.

Finally, there are other lines of work that capture notions of task similarity for meta-learning through proxy measures such as distance between embedded tasks (Achille et al., 2019; Jomaa et al., 2019).

3 Weighted meta-learning

3.1 Setting and objective

Let \mathcal{X} and \mathcal{Y} represent input and output spaces respectively, and define $\mathcal{Z} := \mathcal{X} \times \mathcal{Y}$. Suppose we have J independently drawn *source* tasks $\{Z^{(j)}\}_{j=1}^J$, where the j -th task $Z^{(j)} := \{z_i^{(j)}\}_{i=1}^{N^{(j)}}$ is defined by a set of data points $z_i^{(j)} \in \mathcal{Z}$. We assume the instances $\{z_i^{(j)}\}$ of a source j are drawn i.i.d. from some unknown distribution $\mathbb{S}^{(j)}$ and that the distributions of the source tasks may be different.

The objective is to use the source tasks to learn an initial model, $f : \mathcal{X} \rightarrow \mathcal{Y}$, that generalizes well with respect to a loss function $\ell : \mathcal{Y} \times \mathcal{Y} \rightarrow \mathbb{R}$ and an unknown *target* distribution \mathbb{T} over $\mathcal{X} \times \mathcal{Y}$. That is, the expected target risk $\mathbb{E}_{\mathbb{T}} \ell(y, f(x))$ is small.

Importantly, we assume that a small i.i.d. sample from the target distribution, $Z^T = \{z_i^T\}_{i=1}^{N^{(T)}}$, is available and can be utilized during training, where $N^{(T)} \ll N^{(j)}$, for all $1 \leq j \leq J$. In the model-agnostic meta-learning (MAML) framework of Finn et al. (2017), the target sample is utilized during a “fast adaptation” phase after learning an initial model but prior to prediction on the target task. In contrast, rather than using only the source tasks during meta-training, we additionally use this labeled target sample Z^T to learn the initial model.

In the following, let δ_z denote the Dirac measure at $z \in \mathcal{Z}$. Denote the j -th empirical source distribution and the empirical target distribution by

$$\hat{\mathbb{S}}^{(j)} := \frac{1}{N^{(j)}} \sum_{i=1}^{N^{(j)}} \delta_{z_i^{(j)}}, \quad \hat{\mathbb{T}} := \frac{1}{N^{(T)}} \sum_{i=1}^{N^{(T)}} \delta_{z_i^T},$$

respectively. Given weights $\alpha \in \Delta^{J-1} := \{\alpha \in [0, 1]^J : \sum_{j=1}^J \alpha_j = 1\}$, we define the empirical α -mixture distribution among the J source samples as $\hat{\mathbb{S}}_\alpha := \sum_{j=1}^J \alpha_j \hat{\mathbb{S}}^{(j)}$.

With this notation, the empirical risk of a model on a source task is given by $\mathbb{E}_{\hat{\mathbb{S}}^{(j)}} \ell(y, f(x))$, the empirical risk on the target task by $\mathbb{E}_{\hat{\mathbb{T}}} \ell(y, f(x))$, and the empirical risk on an α -mixture of source samples by $\mathbb{E}_{\hat{\mathbb{S}}_\alpha} \ell(y, f(x))$.

Let \mathcal{G} be a function class with members mapping from \mathcal{Z} to \mathbb{R} . We consider a class of meta-learning algorithms that learns the initial model by minimizing the following task-weighted meta-objective:

$$\sum_{j=1}^J \alpha_j \mathbb{E}_{\hat{\mathbb{S}}^{(j)}} g(z), \quad (1)$$

where $\alpha \in \Delta^{J-1}$. Let $\ell : \mathcal{Y} \times \mathcal{Y} \rightarrow \mathbb{R}$ denote a loss function and $\mathcal{F} = \{f(x; \theta) : \theta \in \Theta\}$ denote a parameterized predictor or model class with $f(\cdot; \theta) : \mathcal{X} \rightarrow \mathcal{Y}$. Joint training (i.e., standard ERM with uniform weights on the tasks) is instantiated in this framework with uniform weights $\alpha_j = 1/J$ and the function class

$$\mathcal{G} = \{g(x, y) = \ell(y, f(x; \theta)) : \theta \in \Theta\}. \quad (2)$$

MAML is instantiated with $\alpha_j = 1/J$ and

$$\mathcal{G} = \{g(x, y) = \ell(y, f(x; U(\theta))) : \theta \in \Theta\}, \quad (3)$$

where U is an adaptation function defined by

$$U(\theta) := \theta - \eta \nabla_{\theta} \mathbb{E}_{\hat{\mathbb{S}}_{\alpha}} \ell(y, f(x; \theta))$$

and η is a global step-size parameter.

In this work, we will explicitly consider the function classes in Equation (2) and Equation (3) with non-uniform weights $\alpha \in \Delta^{J-1}$, but other function classes can also be considered in this framework, including the gradient-based meta-learning methods first-order MAML and Reptile (Nichol et al., 2018). However, note that the bound presented in Theorem 3.4 applies to general classes of functions \mathcal{G} mapping \mathcal{Z} to \mathbb{R} .

Given the objective of Equation (1), it might be natural to upweight source tasks that are more similar to the target task. In particular, we will use an integral probability metric (IPM) (Müller, 1997) as a measure of distance between the distributions of the weighted sources and the target.

Definition 3.1. *The integral probability metric (IPM) between two probability distributions \mathbb{P} and \mathbb{Q} on \mathcal{Z} with respect to the class of real-valued functions \mathcal{G} is defined as*

$$\gamma_{\mathcal{G}}(\mathbb{P}, \mathbb{Q}) := \sup_{g \in \mathcal{G}} |\mathbb{E}_{\mathbb{P}} g(z) - \mathbb{E}_{\mathbb{Q}} g(z)|. \quad (4)$$

Many popular metrics between probability distributions can be cast in terms of an IPM with respect to a specific class of functions \mathcal{G} , such as the total variation distance, the Wasserstein distance, the bounded Lipschitz distance, and the kernel distance (c.f. Sriperumbudur et al. (2012, Table 1)).

The IPM has been applied to function classes involving a parameterized model f in a number of different contexts, including domain adaptation (Zhang et al., 2012). The IPM also describes the discrepancy distance of Mansour et al. (2009a) (c.f. Adlam et al. (2019, Section 2)) for comparing distributions defined on the input space \mathcal{X} , and other IPMs between distributions on \mathcal{X} have been used for learning in generative adversarial networks (Zhang et al., 2018). The discrepancy distance of Mansour et al. (2009a) is itself a generalization of the \mathcal{H} -divergence of Ben-David et al. (2010) from 0-1 loss to arbitrary losses. We refer to Zhang et al. (2013, Sec. 3.2) for additional discussion of these relationships.

In Section 4, we provide a computable algorithm for finding the α weight values, based on computing the IPM between source and target samples with respect to the class of functions consisting of the composition of the loss and model class.

3.2 Data-dependent bound for weighted meta-learning

We now provide a data-dependent upper bound on the distance between the empirical risk of an α -mixture of source tasks and the expected risk of the target task, where the bound holds uniformly over the class of functions \mathcal{G} : that is, we upper bound the quantity

$$\gamma_{\mathcal{G}}(\hat{\mathbb{S}}_{\alpha}, \mathbb{T}) = \sup_{g \in \mathcal{G}} \left| \sum_{j=1}^J \alpha_j \mathbb{E}_{\hat{\mathbb{S}}^{(j)}} g(z) - \mathbb{E}_{\mathbb{T}} g(z) \right|. \quad (5)$$

The bound directly yields (i) a generalization bound for target risk in terms of an empirical IPM between weighted source samples and the target sample and (ii) a computable algorithm for finding the weights α that minimize the bound.

We first present a definition and corresponding result that will be used for our bound.

Definition 3.2. *The empirical Rademacher complexity of a function class \mathcal{G} with respect to a sample $\{z_i\}_{i=1}^N$ drawn i.i.d. from a distribution \mathbb{P} is defined as*

$$\mathcal{R}(\mathcal{G}|z_1, \dots, z_N) := \mathbb{E} \sup_{g \in \mathcal{G}} \frac{1}{N} \left| \sum_{i=1}^N \sigma_i g(z_i) \right|,$$

where the expectation is taken w.r.t. the i.i.d. Rademacher random variables $\{\sigma_i\}$. The expected Rademacher complexity is defined as

$$\mathcal{R}(\mathcal{G}) := \mathbb{E}_{\mathbb{P}^N} \mathcal{R}(\mathcal{G}|z_1, \dots, z_N),$$

where \mathbb{P}^N denotes an N -fold product distribution of \mathbb{P} .

The following is a standard uniform deviation bound based on Rademacher complexity (c.f. Bartlett and Mendelson (2002)):

Lemma 3.3 (Uniform deviation with empirical Rademacher complexity). *Let the sample $\{z_1, \dots, z_N\}$ be drawn i.i.d. from a distribution \mathbb{P} over \mathcal{Z} and let \mathcal{G} denote a class of functions on \mathcal{Z} with members mapping from \mathcal{Z} to $[a, b]$. Then for $\epsilon > 0$, we have that with probability at least $1 - \epsilon$ over the draw of the sample,*

$$\sup_{g \in \mathcal{G}} \left| \mathbb{E}_{\hat{\mathbb{P}}} g(z) - \mathbb{E}_{\mathbb{P}} g(z) \right| \leq 2 \mathcal{R}(\mathcal{G}|z_1, \dots, z_N) + 3 \sqrt{\frac{(b-a)^2 \log(2/\epsilon)}{2N}}, \quad (6)$$

where $\hat{\mathbb{P}}$ represents the empirical distribution of the sample, and $\mathcal{R}(\mathcal{G}|z_1, \dots, z_N)$ denotes the empirical Rademacher complexity of the function class \mathcal{G} w.r.t. the sample.

Our main result is the following data-dependent upper bound on $\gamma_{\mathcal{G}}(\hat{\mathbb{S}}_{\alpha}, \mathbb{T})$, which decomposes into a sum of the IPM between the empirical distribution of the α -mixture of sources $\hat{\mathbb{S}}_{\alpha}$ and empirical target distribution $\hat{\mathbb{T}}$ and the empirical Rademacher complexity with respect to the target distribution.

Theorem 3.4. *Let \mathcal{G} denote a class of functions whose members map from \mathcal{Z} to $[a, b]$, and suppose that the source tasks $\{Z^{(j)}\}_{j=1}^J$ and target task Z^T are independent, and that the data instances of each are i.i.d. within a sample. Let $\epsilon > 0$. Then with probability at least $1 - \epsilon$ over the draws of the source and target samples,*

$$\gamma_{\mathcal{G}}(\hat{\mathbb{S}}_{\alpha}, \mathbb{T}) \leq \gamma_{\mathcal{G}}(\hat{\mathbb{S}}_{\alpha}, \hat{\mathbb{T}}) + 2\mathcal{R}(\mathcal{G}|z_1, \dots, z_{N^{(T)}}) + 3 \sqrt{\frac{(b-a)^2 \log(2/\epsilon)}{2N^{(T)}}}, \quad (7)$$

where $\mathcal{R}(\mathcal{G}|z_1, \dots, z_{N^{(T)}})$ denotes the empirical Rademacher complexity of the function class \mathcal{G} w.r.t. the target sample.

Proof. With probability 1 over the draw of target sample, we have

$$\begin{aligned} \gamma_{\mathcal{G}}(\hat{\mathbb{S}}_{\alpha}, \mathbb{T}) &= \sup_{g \in \mathcal{G}} \left| \mathbb{E}_{\hat{\mathbb{S}}_{\alpha}} g(z) + \mathbb{E}_{\hat{\mathbb{T}}} g(z) - \mathbb{E}_{\hat{\mathbb{T}}} g(z) - \mathbb{E}_{\mathbb{T}} g(z) \right| \\ &\leq \sup_{g \in \mathcal{G}} \left[\left| \mathbb{E}_{\hat{\mathbb{S}}_{\alpha}} g(z) - \mathbb{E}_{\hat{\mathbb{T}}} g(z) \right| + \left| \mathbb{E}_{\hat{\mathbb{T}}} g(z) - \mathbb{E}_{\mathbb{T}} g(z) \right| \right] \\ &\leq \sup_{g \in \mathcal{G}} \left| \mathbb{E}_{\hat{\mathbb{S}}_{\alpha}} g(z) - \mathbb{E}_{\hat{\mathbb{T}}} g(z) \right| + \sup_{g \in \mathcal{G}} \left| \mathbb{E}_{\hat{\mathbb{T}}} g(z) - \mathbb{E}_{\mathbb{T}} g(z) \right| \\ &= \gamma_{\mathcal{G}}(\hat{\mathbb{S}}_{\alpha}, \hat{\mathbb{T}}) + \sup_{g \in \mathcal{G}} \left| \mathbb{E}_{\hat{\mathbb{T}}} g(z) - \mathbb{E}_{\mathbb{T}} g(z) \right|, \end{aligned}$$

where in the first inequality, we applied the triangle inequality, the second inequality, we split the supremum terms, and in the last line, we applied Definition 3.1.

The term $\sup_{g \in \mathcal{G}} \left| \mathbb{E}_{\hat{\mathbb{T}}} g(z) - \mathbb{E}_{\mathbb{T}} g(z) \right|$ can be bounded in a variety of ways. Here, we use a standard bound via the empirical Rademacher complexity (Lemma 3.3) to yield the result. \square

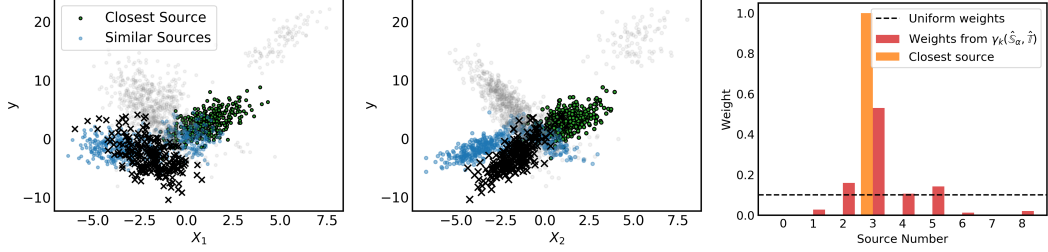


Figure 1: 2-dimensional data sampled from isotropic Gaussian distributions. **Left, Middle:** The black x's denote a target task, and the green points denote the closest source, which receives full weight when minimizing a bound based on Corollary 3.5. The blue sources denote other sources that receive greater than $1/J$ weight when minimizing the bound based on Theorem 3.4, where J is the number of sources, and the gray black circles denote the remaining sources that have weight less than $1/J$. **Right:** The respective weightings from minimizing the bounds based on Theorem 3.4 and Corollary 3.5.

The bound in Theorem 3.4 involves purely empirical quantities, i.e., the empirical IPM and empirical Rademacher complexity. Note that only the empirical IPM in the first term involves the α -weights.

Since $\alpha \in \Delta^{J-1}$, it follows that

$$\begin{aligned}
 \gamma_{\mathcal{G}}(\hat{\mathbb{S}}_{\alpha}, \hat{\mathbb{T}}) &= \sup_{g \in \mathcal{G}} \left| \sum_{j=1}^J \alpha_j \mathbb{E}_{\hat{\mathbb{S}}^{(j)}} g(z) - \mathbb{E}_{\hat{\mathbb{T}}} g(z) \right| \\
 &\leq \sup_{g \in \mathcal{G}} \sum_{j=1}^J \alpha_j \left| \mathbb{E}_{\hat{\mathbb{S}}^{(j)}} g(z) - \mathbb{E}_{\hat{\mathbb{T}}} g(z) \right| \\
 &\leq \sum_{j=1}^J \alpha_j \sup_{g \in \mathcal{G}} \left| \mathbb{E}_{\hat{\mathbb{S}}^{(j)}} g(z) - \mathbb{E}_{\hat{\mathbb{T}}} g(z) \right| \\
 &= \sum_{j=1}^J \alpha_j \gamma_{\mathcal{G}}(\hat{\mathbb{S}}^{(j)}, \hat{\mathbb{T}}).
 \end{aligned}$$

This immediately yields the corollary:

Corollary 3.5. *Assume the conditions of Theorem 3.4 hold. Then with probability at least $1 - \epsilon$,*

$$\gamma_{\mathcal{G}}(\hat{\mathbb{S}}_{\alpha}, \mathbb{T}) \leq \sum_{j=1}^J \alpha_j \gamma_{\mathcal{G}}(\hat{\mathbb{S}}^{(j)}, \hat{\mathbb{T}}) + 2\mathcal{R}(\mathcal{G}|z_1, \dots, z_{N^{(\tau)}}) + 3\sqrt{\frac{(b-a)^2 \log(2/\epsilon)}{2N^{(\tau)}}}. \quad (8)$$

While the weighted empirical IPM in Corollary 3.5 results in a looser bound, it leads to an even simpler and computationally cheaper weight selection rule, which may be sufficient for some problems; we discuss this further in Section 4.

Corollary 3.5 can be interpreted as an empirical version of the bound in Zhang et al. (2013, Theorem 5.2) for the function class \mathcal{G} defined in Equation (2); in Zhang et al. (2013, Theorem 5.2), the upper bound on $\gamma_{\mathcal{G}}(\hat{\mathbb{S}}_{\alpha}, \mathbb{T})$ includes a population IPM with respect to \mathcal{G} and a weighted sum of expected Rademacher complexity terms on the source domains.

In Figure 1, we show an example of a 2-dimensional regression task with 9 source tasks, each generated from an isotropic Gaussian distribution. In the two leftmost figures, the dark black points represent the target task, and the green points represent the most similar task. Minimizing a bound based on Corollary 3.5 is equivalent to putting all weight on the closest task. By contrast, minimizing the bound based on Theorem 3.4, allows for finding the best mixture of source tasks such that this mixture is close to the target; the additional source tasks with weight greater than $1/J$ are highlighted in blue (in addition to the source in green). The weights found by minimizing a kernel distance (see Section 4) are plotted in the rightmost graph.

4 Algorithm for weight selection using empirical kernel distances

The upper bounds given in Theorem 3.4 and Corollary 3.5 lead naturally to an algorithm for computing the weights by minimizing the bound. However, optimizing the upper bound of Theorem 3.4 or Corollary 3.5 requires computing the IPM $\gamma_{\mathcal{G}}(\hat{\mathbb{S}}_{\alpha}, \hat{\mathbb{T}})$ or IPMs $\{\gamma_{\mathcal{G}}(\hat{\mathbb{S}}^{(j)}, \hat{\mathbb{T}})\}_{j=1}^J$, which are in general not computable for arbitrary function classes \mathcal{G} (Sriperumbudur et al., 2012). Thus, the goal is to compute a surrogate distance that provides an upper bound on the empirical IPMs.

4.1 The kernel distance

One candidate for such a surrogate distance is the kernel distance, which is an integral probability metric defined with respect to the class of functions given by the unit ball of a reproducing kernel Hilbert space (RKHS), i.e., $\mathcal{G}_{\text{RKHS}} := \{g : \|g\|_{\mathcal{K}_k} \leq 1\}$, where \mathcal{K}_k is a Hilbert space associated with a reproducing kernel $k : \mathcal{Z} \times \mathcal{Z} \rightarrow \mathbb{R}$ and $\|\cdot\|_{\mathcal{K}_k}$ is the norm induced by the inner product on \mathcal{K}_k . That is, the Hilbert space \mathcal{K}_k associated with a reproducing kernel k has the properties that (1) for all $z \in \mathcal{Z}$, $k(\cdot, z) \in \mathcal{K}_k$ and (2) for all $z \in \mathcal{Z}$ and for all functions $g \in \mathcal{K}_k$, $g(z) = \langle g, k(\cdot, z) \rangle_{\mathcal{K}_k}$.

Let $\gamma_{\mathcal{G}_{\text{RKHS}}}(\mathbb{P}, \mathbb{Q})$ denote the kernel distance with respect to the probability distributions \mathbb{P} and \mathbb{Q} . In order to upper bound the IPMs defined with respect to \mathcal{G} , we need to find an RKHS ball $\mathcal{G}_{\text{RKHS}}$ associated with a kernel k such that the function class is contained in the RKHS ball, i.e., $\mathcal{G} \subseteq \mathcal{G}_{\text{RKHS}}$. Then respective IPMs can then be bounded as

$$\gamma_{\mathcal{G}}(\hat{\mathbb{S}}_{\alpha}, \hat{\mathbb{T}}) \leq \gamma_{\mathcal{G}_{\text{RKHS}}}(\hat{\mathbb{S}}_{\alpha}, \hat{\mathbb{T}}) := \gamma_k(\hat{\mathbb{S}}_{\alpha}, \hat{\mathbb{T}}) \quad (9)$$

and for $1 \leq j \leq J$,

$$\gamma_{\mathcal{G}}(\hat{\mathbb{S}}^{(j)}, \hat{\mathbb{T}}) \leq \gamma_{\mathcal{G}_{\text{RKHS}}}(\hat{\mathbb{S}}^{(j)}, \hat{\mathbb{T}}) := \gamma_k(\hat{\mathbb{S}}^{(j)}, \hat{\mathbb{T}}), \quad (10)$$

where $\gamma_k(\cdot, \cdot)$ is the empirical kernel distance, or maximum mean discrepancy.

The empirical kernel distance between the α -weighted source distribution and the target distribution $\gamma_k(\hat{\mathbb{S}}_{\alpha}, \hat{\mathbb{T}})$ can be easily computed (Sriperumbudur et al. (2012, Theorem 2.4)) as

$$\gamma_k(\hat{\mathbb{S}}_{\alpha}, \hat{\mathbb{T}}) = \sqrt{v_{\alpha}^{\top} K_J v_{\alpha}}, \quad v_{\alpha} := \left[\frac{\alpha_1}{N^{(1)}}, \dots, \frac{\alpha_J}{N^{(J)}}, \frac{-1}{N^{(T)}} \right]^{\top} \in \mathbb{R}^{J+1}, \quad (11)$$

where $K_J \in \mathbb{R}^{(J+1) \times (J+1)}$ is a kernel gram matrix between tasks, with $[K_J]_{j,j'} = \sum_{i,i'} k(z_i^{(j)}, z_{i'}^{(j')})$. The empirical kernel distance for a single source and target distribution can then be computed as $\gamma_k(\hat{\mathbb{S}}^{(j)}, \hat{\mathbb{T}}) = \gamma_k(\hat{\mathbb{S}}_{e_j}, \hat{\mathbb{T}})$, where $e_j \in \Delta^{J-1}$ is the j -th standard basis vector.

Minimizing a bound based on the kernel distance in Equation (11) involves solving a quadratic program with simplex constraints, which has time complexity $O(J^3)$ when the gram matrix K_J is positive definite. Finally, an even simpler approach than optimizing a bound based on Theorem 3.4 (via Equation (11)) is optimizing a bound based on Corollary 3.5, which only requires computing each the distances $\{\gamma_k(\hat{\mathbb{S}}^{(j)}, \hat{\mathbb{T}})\}_{j=1}^J$ once and reporting the minimum distance.

4.2 Upper bounds on the IPM for linear basis models

We have established that if $\mathcal{G} \subseteq \mathcal{G}_{\text{RKHS}}$, then the IPM $\gamma_{\mathcal{G}}$ with respect to \mathcal{G} can be upper bounded with a computable empirical kernel distance γ_k with respect to the RKHS ball $\mathcal{G}_{\text{RKHS}}$, as in Equation (9) and Equation (10). We now show how to construct a class of functions $\mathcal{G}_{\text{RKHS}}$ such that $\mathcal{G} \subseteq \mathcal{G}_{\text{RKHS}}$ for regression and binary classification settings; concretely, we consider linear basis models with square loss and hinge loss functions, respectively.

Let $\psi : \mathcal{X} \rightarrow \mathbb{R}^d$ denote a basis function, and consider the class of linear basis function models composed with a loss ℓ ,

$$\mathcal{G}^{\ell} := \{g((x, y)) = \ell(y, w^{\top} \psi(x; \theta)) : w \in \mathcal{W}, \theta \in \Theta\},$$

where $\mathcal{W} \subset \mathbb{R}^d$ denotes a constraint set and Θ denotes the parameter space for the basis function ψ . We consider selecting kernels for the class of functions \mathcal{G}^{ℓ} such that $\mathcal{G}^{\ell} \subseteq \mathcal{G}_{\text{RKHS}}$, where $\mathcal{G}_{\text{RKHS}}$ is a RKHS ball associated with the kernel. To do so, we define a feature map ϕ mapping \mathbb{R}^{d+1} to a

Euclidean feature space, and define $\mathcal{G}_{\text{RKHS}}$ to be a ball of an RKHS \mathcal{K}_k constructed from the kernel $k(z, z') = \langle \phi(\psi(x), y), \phi(\psi(x'), y') \rangle$.

In the following, let z denote a point $(\psi(x), y)$, and let $\text{vec}(\cdot)$ denote the vectorization operator. First we consider the class of functions \mathcal{G}^ℓ when ℓ is a square loss function.

Lemma 4.1 (Square loss). *Let $\mathcal{W} = \{w \in \mathbb{R}^d : \|w\|_2 \leq 1\}$. For $\ell(y, y') = \frac{1}{2}(y - y')^2$, construct an RKHS from the feature map $\phi : \mathbb{R}^{d+1} \rightarrow \mathbb{R}^{d^2+d+1}$,*

$$\phi((\psi(x), y)) = \begin{pmatrix} \text{vec}(\psi(x)\psi(x)^\top) \\ \sqrt{2}y\psi(x) \\ y^2 \end{pmatrix}.$$

Then, $\mathcal{G}^\ell \subseteq \mathcal{G}_{\text{RKHS}}$ for the kernel k associated with the feature map ϕ .

Proof. Fix $w \in \mathcal{W}$ and let $a_1 = \frac{1}{2}$, $z_1 = (-w, 1)$. Let $g \in \mathcal{G}^\ell$. Then

$$\begin{aligned} g(z) &= \ell(y, w^\top \psi(x)) \\ &= \frac{1}{2}(w^\top \psi(x) - y)^2 \\ &= \frac{1}{2}(\text{vec}(\psi(x)\psi(x)^\top)^\top \text{vec}(ww^\top) - 2y\psi(x)^\top w + y^2) \\ &= a_1 \phi(z)^\top \phi(z_1) = a_1 k(z, z_1) \in \mathcal{K}_k. \end{aligned} \tag{12}$$

Applying Equation (12) and Property (2) of the RKHS, g has bounded norm:

$$\|g\|_{\mathcal{K}_k}^2 = \langle g, g \rangle_{\mathcal{K}_k} = a_1 \langle g, k(\cdot, z_1) \rangle_{\mathcal{K}_k} = a_1^2 k(z_1, z_1) = a_1^2 (\|w\|_2^2 + 2\|w\|_2 + 1) \leq 1,$$

where the inequality follows from the assumption that $\|w\|_2 \leq 1$. Thus, $\mathcal{G}^\ell \subseteq \mathcal{G}_{\text{RKHS}}$. \square

Now we consider \mathcal{G}^ℓ where ℓ is a hinge loss function, with constraints on the domain and parameter spaces. This allows us to, e.g., utilize a penalized SVM with sufficiently small penalty C on the solution norm, i.e., $\|w\|^2 \leq C$.

Lemma 4.2 (Hinge loss). *Let $\mathcal{W} = \{w \in \mathbb{R}^d : \|w\|_2 \leq 1\}$, $\Theta = \{\theta : \|\psi(x; \theta)\|_2 \leq 1\}$, $\mathcal{Y} = [-1, 1]$. Under the constraints on the input and output spaces,*

$$\ell(y, y') = \max(1 - y\psi(x)^\top w, 0) = 1 - y\psi(x)^\top w.$$

Construct an RKHS from the feature map $\phi : \mathbb{R}^{d+1} \rightarrow \mathbb{R}^{d+1}$,

$$\phi((\psi(x), y)) = \begin{pmatrix} y\psi(x) \\ 1 \end{pmatrix}.$$

Then, $\mathcal{G}^\ell \subseteq \mathcal{G}_{\text{RKHS}}$ for the kernel k associated with the feature map ϕ .

Proof. Fix $w \in \mathcal{W}$ and let $z_1 = (-w, 1)$. Let $g \in \mathcal{G}^\ell$. Then, g is an element of the RKHS \mathcal{K}_k , i.e.,

$$g(z) = \ell(y, w^\top \psi(x)) = 1 - y\psi(x)^\top w = k(z, z_1) \in \mathcal{K}_k,$$

which, along with Property (2) of the RKHS, implies that g has bounded norm:

$$\|g\|_{\mathcal{K}_k}^2 = \langle g, g \rangle_{\mathcal{K}_k} = \langle g, k(\cdot, z_1) \rangle_{\mathcal{K}_k} = k(z_1, z_1) = \|w\|_2^2 + 1 \leq 2,$$

where we applied the assumption that $\|w\|_2 \leq 1$. Thus, $\mathcal{G}^\ell \subseteq \mathcal{G}_{\text{RKHS}}$. \square

Note that in Lemma 4.2, $\mathcal{G}_{\text{RKHS}}$ is a $\sqrt{2}$ -RKHS ball; the extra constant factor only scales the kernel distance computation and therefore does not affect the computation of the weights.

Thus, since the upper bounds on the empirical IPM in Equation (9) and Equation (10) hold for linear basis functions with square and hinge loss, we can apply a weight minimization algorithm based on minimizing the kernel distance, instead of the IPMs in Theorem 3.4 and Corollary 3.5.

This construction encodes a natural notion for task similarity: when the kernel distance between two tasks is relatively small, this implies that the model class cannot distinguish between these tasks with respect to the associated loss function. Hence, a model learned on one task should perform similarly on the other task.

Algorithm 1 Meta-training procedure for α -meta-learning

- 1: **Input:** kernel k , source tasks $\{Z_j\}_{j=1}^J$, target task Z^T
 - 2: Compute empirical kernel distance $\gamma_k(\hat{S}_\alpha, \hat{T}) = \sqrt{v_\alpha^\top K_J v_\alpha}$
 - 3: Compute $\hat{\alpha} := \arg \min_{\alpha \in \Delta^{J-1}} \gamma_k(\hat{S}_\alpha, \hat{T})$
 - 4: Learn initial model by minimizing $\sum_{j=1}^J \hat{\alpha}_j \mathbb{E}_{\hat{S}_\alpha^{(j)}} g(z)$
 - 5: **Output:** weights $\hat{\alpha}$ and initial model \hat{g}
-

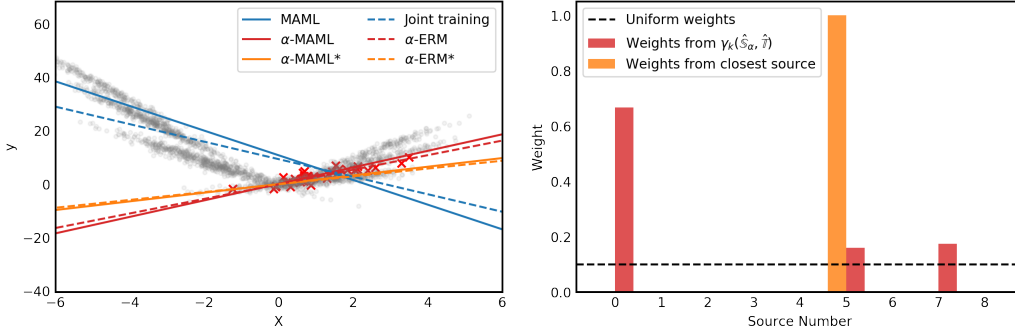


Figure 2: **Left:** Linear regression with MAML, joint training, α -MAML, and α -ERM solutions. Red x 's denote the target task, and gray points denote the 9 source tasks. **Right:** The various weightings obtained from uniform weighting, α -weighting according to the kernel IPM between the α -mixture of sources and target, or weighting only the closest source.

4.3 Weighted meta-learning for linear basis models

The examples in Section 4.2 examine classes of linear basis functions composed with a loss \mathcal{G}^ℓ without explicitly considering an adaptation function U . Finn et al. (2019) summarizes sufficient conditions of under which the projection in Section 3.1 is equivalent to a contraction, ensuring that model updates during training remain within \mathcal{G}^ℓ . More generally, a projection step back into \mathcal{G}^ℓ can be utilized during optimization.

Algorithm 1 summarizes the meta-learning procedure used learn the α weight values and an initial model. Note that in an adaptive basis setup, steps 2–4 are iterated, since selecting g changes the basis function ψ .

5 Experiments

We present several regression examples on synthetic and real data tasks that use α -weighted meta-learning and compare to the uniformly-weighted setting, which recovers algorithms such as MAML and joint training. Additional experimental details can be found in Appendix A.

5.1 Synthetic linear regression

First we examine a 1-dimensional linear regression setting. We generated 9 source tasks and 1 target task as follows. The task sizes were generated according to a multinomial distribution with a uniform prior on the multinomial parameter. For each source, the covariates were generated from a gaussian with mean μ_j and variance 1, where $\mu_j \sim \text{uniform}(-5, 5)$. The slope of the j -th task was set to $2\mu_j$, and the response of the j -th source was then drawn according to $y_j \sim 2\mu_j + \epsilon$, where $\epsilon \sim \mathcal{N}(0, 1)$.

We note that for weighted MAML and weighted ERM, an analytical solution to the meta-objective can be computed, see Appendix A.1 for a derivation. Thus, the analytical solution is used to compute an initialization, and we compare the resulting initializations from α -weighted meta-learning and uniform weighting. All MAML solutions were computed with $\eta = 0.0001$ step size.

In Figure 2, we plot the initializations obtained from each method. Here α -MAML and α -ERM denote the initializations from minimizing the bound with the kernel distance, whereas α -MAML*

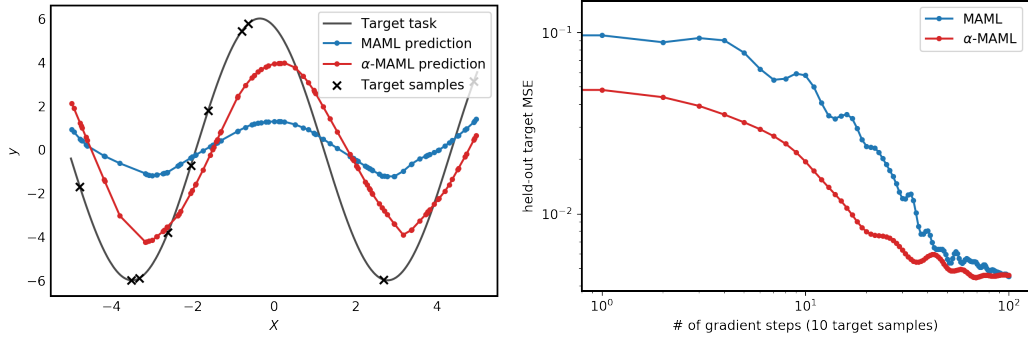


Figure 3: Sine wave regression with 10 labeled target examples. **Left:** Predictions after training MAML and weighted MAML for 10,000 meta-iterations. **Right:** Held-out target mean squared error after L gradient steps of fast adaptation.

and α -ERM* denote the initializations obtained from placing all weight on the closest source. The kernel distance was computed using 20 target training examples (denoted by red points). Lines denote inferred hypotheses using uniform, α , and closest source weightings. We observe that the uniformly-weighted initializations (blue) correspond to an average model learned from all the sources, whereas unequally weighted sources (red, orange) are able to use the task similarity to better represent the target task. The weights are shown in the bottom plot in Figure 2, where the weights obtained from minimizing the kernel distance $\gamma_k(\hat{S}_\alpha, \hat{T})$ place weight on 3 sources.

5.2 Sine regression with α -MAML

We generated synthetic sine wave tasks as follows. The target task was assigned a fixed amplitude of 6 with a small number of samples (5, 10, 20) for training and fast adaptation, and 100 data points were randomly sampled from the target task for evaluation. For the source tasks, the amplitudes were drawn according to a gamma(1, 2) distribution. For both target and source tasks, the phase parameter was drawn uniformly from $(0, \pi)$, as in the setup in Finn et al. (2017). From each source task, 40 samples were drawn, where the x values were sampled uniformly from $(-5, 5)$.

Following Finn et al. (2017), we used a fully-connected neural network with 2 hidden layers of size 40 with ReLU non-linearities. For all experiments, Adam was used as the meta-optimizer with an inner-loop learning rate of 0.01 and an outer-loop learning rate of 0.001. In each iteration of weighted MAML, we sample a mini-batch of T tasks, compute embeddings for T tasks and the target task, compute weights by optimizing the bound (and computing kernel distances using the computed embeddings of the sources and target), compute weighted loss using the optimal weights, and lastly, update the model parameters. We used the same as above for MAML but with uniformly weighted source tasks. For both MAML and weighted MAML, the mini-batch size was set to $T = 100$ tasks.

Figure 3 shows one target task where 10 training samples (denoted by black points) are drawn from the target (denoted by the solid black curve). The red and blue curves denote the resulting predictions from the learned initializations of uniformly-weighted MAML and α -weighted MAML. In the bottom plot, the initializations are adapted to the 10 target samples. In this plot, we observe that only after a larger number of gradient steps (~ 100) is the uniform weighting able to achieve a comparable mean squared error on the held-out target samples as the α -weighted initialization.

In Table 1, we report the average RMSE for each method before and after fast adaptation for MAML and ERM with 1) uniform weights, 2) α -weights (Algorithm 1), and 3) threshold weights (i.e., closest source selection). In the table, we see that the predictions from the initializations are fairly close for all methods, with the threshold method and α -MAML achieving lower RMSE on the predicted values than uniformly-weighted MAML on average. On average, the α -MAML is able to adapt better in 10 gradient steps than the uniformly and single-source threshold MAML initializations, and the threshold method still is competitive for fast adaptation, especially relative to uniformly weighted MAML.

Table 1: RMSE of sine wave predictions using (1) the initial meta-model and (2) after 10 gradient steps (denoted by †) for 5-shot, 10-shot, and 20-shot target training scenarios, averaged over 4 random trials.

	5-shot	10-shot	20-shot
MAML	3.90 ± 0.85	3.57 ± 0.66	4.11 ± 0.94
α -MAML	3.21 ± 1.12	2.93 ± 0.75	3.05 ± 1.09
Threshold	2.83 ± 1.04	3.17 ± 1.05	3.26 ± 1.08
MAML [†]	4.24 ± 1.00	1.90 ± 0.26	2.06 ± 0.39
α -MAML [†]	2.65 ± 1.34	1.68 ± 0.77	1.67 ± 0.75
Threshold [†]	2.35 ± 1.75	2.01 ± 0.83	2.01 ± 0.88

Table 2: RMSE of initializations for linear regression on sources and target using 20 labeled target training examples to compute the weights (before fast adaptation).

	Diabetes	Boston
MAML	50.44	3.64
α -MAML	49.36	3.59
Joint training	50.31	3.58
α -ERM	49.24	3.32
target	92.31	15.47

5.3 Weighted meta-learning for real data tasks

Multi-dimensional linear regression. We examined two multi-dimensional regression data sets. The first uses the diabetes data set studied by Efron et al. (2004), which contains 10 covariates. The goal is to predict a real-valued response that measures disease progression one year after baseline. We split the data set into separate source tasks by grouping on age, leading to a total of 6 source tasks, using the remaining covariates in each source. We picked a separate age group for the target task, using 20 target samples for computing the kernel distance and the remaining target samples were used for testing.

The second data set is the Boston house prices data of Harrison Jr and Rubinfeld (1978), which includes 13 covariates, and the response variable is the median value of owner-occupied homes. To form sources, we grouped on the attribute age, and separated the full data into 6 source tasks, where each source contained a group of 50 ages, and the remaining 12 covariates were used in each source. The target task contained 30 target samples for training, and the remaining samples were used for testing.

The root mean squared error (RMSE) of each of the initializations obtained are presented in Table 2, where all MAML-related computations used $\eta = 0.0001$ for the step size. This is a setting where predicting on only the target training samples performs quite poorly and using the source data sets improves performance for this particular target task. Furthermore, weighting sources by kernel distance seems to also improve prediction error. We found that typically, similar age ranges were upweighted more than further away age groups.

Basis linear regression. Next we examined the sales data set studied by Tan and San Lau (2014). The data set consists of a collection of products with sales information over 52 weeks. We included the 300 products as source tasks, and used a single product as the target task. For the target task, we used the first 10 weeks as labeled target training data, and the last 42 weeks as test data for evaluation. We computed random Fourier features (Rahimi and Recht, 2008) for the weeks and used these features when computing the α -weights in the kernel distance.

In Table 3, we report the RMSE on held-out target data for target tasks with 5 and 10 weeks of data, i.e., 5- and 10-shot target tasks, averaged over 20 different product target tasks. In this example, the table shows that predicting on the target data alone performs very poorly but that meta-learning helps improve performance.

Table 3: RMSE of sales data for 5-shot and 10-shot target training sample sizes, where the remaining data was used for evaluation. Mean and standard deviation computed over 20 target tasks.

	5-shot	10-shot
MAML	12.86 ± 3.79	12.69 ± 3.69
α -MAML	2.43 ± 2.09	2.41 ± 1.92
thresh-MAML	2.53 ± 1.94	2.50 ± 2.03
ERM	12.09 ± 3.53	11.92 ± 3.43
α -ERM	2.52 ± 2.21	2.50 ± 2.04
thresh-ERM	2.45 ± 1.81	2.45 ± 1.97
target	83.63 ± 104.07	209.06 ± 378.88

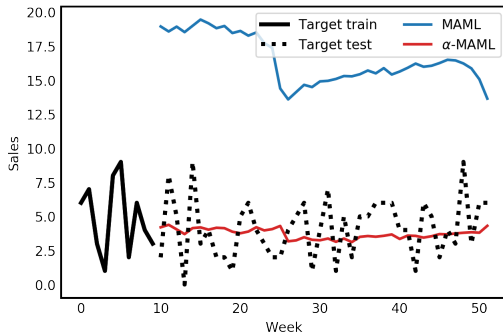


Figure 4: Product sales over 52 weeks. Example target task from the sales data set; the solid black line denotes the data examples used for training, and the dashed black line denotes the data used for testing. The blue and red lines denote the learned initializations (i.e., before fast adaptation).

Here α -MAML and α -ERM are the methods used in Algorithm 1 for MAML and ERM, respectively, whereas thresh-MAML and thresh-ERM correspond to the threshold method that weights the closest source only. In this setting, both weighted methods, i.e., α -based and thresh-based meta-learning, outperform the uniformly-weighted methods.

In Figure 4 we show the learned initializations from α -MAML vs uniformly-weighted MAML, where the learning rate parameter was set as $\eta = 0.0001$. Here the MAML initialization learns a task that is an average of many of the tasks; in contrast, the α -MAML initialization upweights products with more similar sources and patterns as the target. As a result, the α -MAML initialization is able to better predict future data coming from that task.

6 Discussion and future work

We presented a class of weighted meta-learning methods, where the weights are selected by minimizing a data-dependent bound involving an empirical IPM between the weighted sources and target risks. Using this bound, we developed a computable algorithm based on minimizing an empirical kernel distance, providing examples for basis regression models with square loss and hinge loss.

A number of promising future directions remain. One direction is to generalize our approach to arbitrary loss functions, beyond the square and hinge loss, and to extend the method to multi-class classification problems; here it would be necessary to develop additional computational improvements. Additionally, one could consider only use the labeled target task examples during training, but also unlabeled target information to help quickly adapt the tasks. Finally, exploring the use of this method in other applications, such as a continual learning paradigm, remains a fruitful direction.

Acknowledgments

This work was partially completed while Diana Cai was at Microsoft Research New England. Diana Cai is supported in part by a Google Ph.D. Fellowship in Machine Learning.

A Experimental details

In this section, we present additional experimental details and results to complement the results presented in the main paper. In Appendix A.1, we provide a derivation of the analytical solution of weighted MAML and ERM. In Appendix A.2, we discuss an alternative weighted meta-learning algorithm, giving by directly optimizing a generalization bound, and explore the results on the synthetic sine wave regression task. Lastly, we present additional results and details for the experiments considered in Section 5.

A.1 The analytical α -weighted meta-learning solution

The solution to the weighted MAML (and weighted ERM) meta-objective is available in closed form, as we show in this section. We assume a linear model and squared loss for every task. We follow Finn et al. (2019, Appendix A), who provide a derivation of the analytical solution for the uniformly-weighted case of ERM (i.e., joint training) and MAML for linear regression with squared loss.

Denote the MAML adaptation function of the predictors $w \in \mathbb{R}^d$ as

$$U_j(w) := w - \eta(A_j w - b_j),$$

where $A_j := X_j^\top X_j$, $b_j := X_j^\top w$, $X_j \in \mathbb{R}^{N^{(j)} \times d}$ is the covariate matrix of the j -th source task, and $\eta > 0$ is the step size.

The weighted MAML objective can be written as a function of the predictors w as follows

$$\begin{aligned} F(w) &= \sum_{j=1}^J \alpha_j \left(\frac{1}{2} U_j(w)^\top A_j U_j(w) - U_j(w)^\top b_j \right) \\ &= \frac{1}{2} w^\top \left(\sum_{j=1}^J \alpha_j (I - \eta A_j)^\top A_j (I - \eta A_j) \right) w \\ &\quad + w^\top \left(\sum_{j=1}^J \alpha_j (I - \eta A_j)^\top b_j \right). \end{aligned}$$

Defining $\tilde{A}_j := (I - \eta A_j)$, and

$$\tilde{A} := \sum_{j=1}^J \alpha_j \tilde{A}_j^\top A_j \tilde{A}_j, \quad \tilde{b} := \sum_{j=1}^J \alpha_j \tilde{A}_j^\top b_j,$$

we have that the gradient of the meta-objective is

$$\nabla F(w) = \tilde{A} w - \tilde{b},$$

and so the solution is $w_{\alpha\text{-MAML}} = \tilde{A}^{-1} \tilde{b}$.

When the MAML learning rate $\eta = 0$, we recover the solution for the α -weighted ERM, where $U(w) = w$.

A.2 Generalization bound optimization

In Section 4 of the main paper, we describe a high-level algorithm for optimizing for the α weight values, given by

$$\hat{\alpha} := \arg \min_{\alpha \in \Delta^{J-1}} \gamma_k(\hat{\mathbb{S}}_\alpha, \hat{\mathbb{T}}),$$

i.e., minimizing a kernel distance between the empirical distributions of the α -mixture of sources and the target.

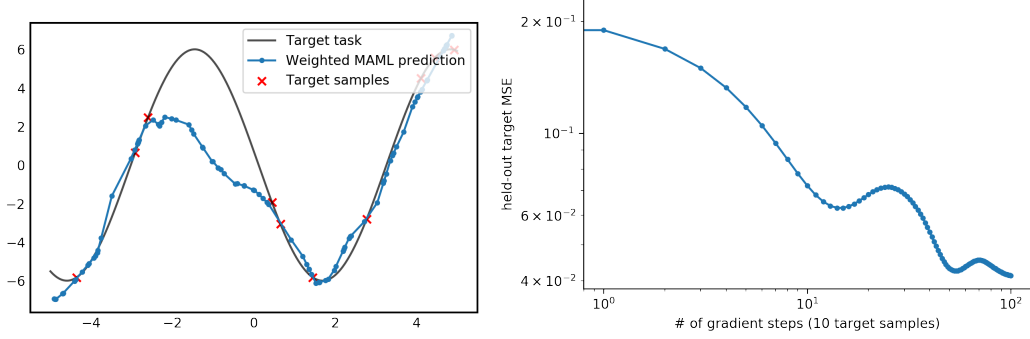


Figure 5: Results of sine wave regression obtained from directly optimizing the generalization bound in Equation (13) during meta-training. **Left:** Learned weighted MAML initialization after 20,000 meta-iterations. **Right:** Held-out MSE after fast adaptation using 10 samples of the target.

An alternative algorithm could also be derived from directly optimizing a generalization bound. Indeed, Theorem 3.4 implies that for all $g \in \mathcal{G}$,

$$\mathbb{E}_{\mathbb{T}}(g) \leq \mathbb{E}_{\hat{\mathbb{S}}_{\alpha}}(g) + \gamma_{\mathcal{G}}(\hat{\mathbb{S}}_{\alpha}, \hat{\mathbb{T}}) + 2\mathcal{R}(\mathcal{G}|z_1, \dots, z_{N(\tau)}) + 3\sqrt{\frac{(b-a)^2 \log(2/\epsilon)}{2N(\tau)}},$$

and similarly, Corollary 3.5 implies that for all $g \in \mathcal{G}$,

$$\mathbb{E}_{\mathbb{T}}(g) \leq \mathbb{E}_{\hat{\mathbb{S}}_{\alpha}}(g) + \sum_{j=1}^J \alpha_j \gamma_{\mathcal{G}}(\hat{\mathbb{S}}^{(j)}, \hat{\mathbb{T}}) + 2\mathcal{R}(\mathcal{G}|z_1, \dots, z_{N(\tau)}) + 3\sqrt{\frac{(b-a)^2 \log(2/\epsilon)}{2N(\tau)}}.$$

Thus, an alternative algorithm to the one proposed in Algorithm 1 would involve directly optimizing the generalization bound above:

$$\hat{\alpha}, \hat{g} := \arg \min_{\alpha \in \Delta^{J-1}, g \in \mathcal{G}} \mathbb{E}_{\hat{\mathbb{S}}_{\alpha}}(g) + \gamma_k(\hat{\mathbb{S}}_{\alpha}, \hat{\mathbb{T}}). \quad (13)$$

We can also propose a variant of the looser bound given by optimizing

$$\hat{\alpha}, \hat{g} := \arg \min_{\alpha \in \Delta^{J-1}, g \in \mathcal{G}} \mathbb{E}_{\hat{\mathbb{S}}_{\alpha}}(g) + \sum_{j=1}^J \alpha_j \gamma_k(\hat{\mathbb{S}}^{(j)}, \hat{\mathbb{T}}). \quad (14)$$

An advantage of optimizing the generalization bound directly rather than the two-step procedure in Algorithm 1 is that we can jointly optimize for the α weight values and model parameters via gradient descent.

We examined the performance of the direct bound optimization above, i.e., optimizing Equation (13) in the sine wave regression setting. We sampled 200,000 source tasks in advance, according to the same task distribution described in Section 5, and used the same 2-layer neural network model as before. Adam was used for the meta-optimizer, with the same learning rates of the main document. In order to speed up the computation, we used mini-batches of size 150. Meta-training was performed for 20,000 meta-iterations.

In Figure 5, we show the results of the direct bound optimization for the sine wave regression example. The top plot shows that the initialization learned is close to the target task, though it does not seem to be able to capture areas where there are no samples as well. By contrast, while the predictions obtained according to Algorithm 1 (see main document, Figure 3) are able to better capture the overall shape of the sine wave task in only 10,000 meta-iterations.

The bottom plot shows that the initialization is able to benefit from fast adaptation, as it can be adapted to the target with a small number of gradient steps; however, the initialization obtained from Algorithm 1 is able to adapt more quickly for this task.

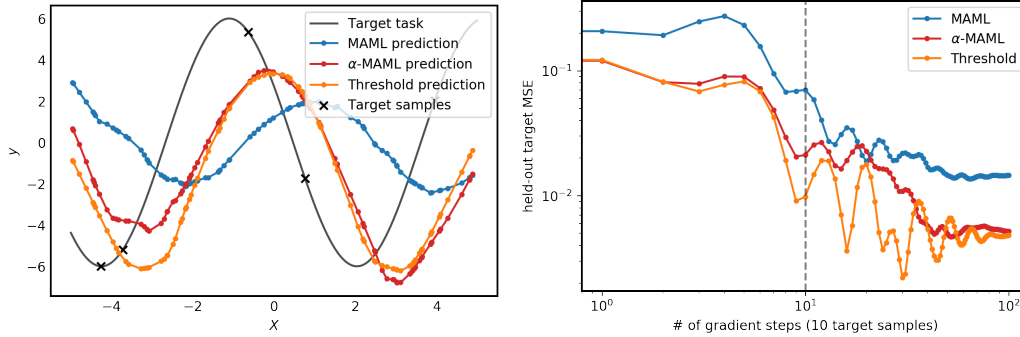


Figure 6: Results of sine wave regression for a 5-shot target task. **Left:** Learned meta-initializations for uniform, α , and single-source weights after 10,000 meta-iterations. **Right:** Target task MSE on 100 held-out target samples after fast adaptation using 5 samples from the target.

Overall, this suggests that the convergence of the direct bound optimization is slower than the α -MAML algorithm of Algorithm 1 for the sine wave regression task. However, the direct bound optimization may still be of interest given enough computational resources, as it is a simpler procedure to implement.

A.3 Sine wave regression

In the main paper, we explored sine regression using an adaptive basis version of Algorithm 1. In particular, we presented plots of a single target and the resulting initializations learned from MAML and α -MAML.

Here we present additional results for 5-shot target training sizes using the adaptive version of Algorithm 1 (based on optimizing an upper bound on Theorem 3.4. We also evaluate a variant that we refer to as the “threshold” meta-learning method, that is based on optimizing an upper bound on Corollary 3.5, which corresponds to weighting only the closest source task.

In each random trial, a random sine task was drawn according to the task distribution described in the main paper, and random samples from the target were also drawn (with fixed amplitude and random phase). Each method was trained for 10,000 meta-iterations. The initializations are evaluated on 1000 held-out samples from each sine task.

In Figure 6, we present a single trial from a 5-shot target task with the learned initializations of each method and the held-out MSE after fast adaptation. In this example, for all methods, fast adaptation helps, implying that the learned meta-initialization is useful for learning this task. However, even after a large number of target tasks, the uniformly-weighted MAML initialization is unable to achieve the same MSE as the non-uniformly weighted initializations (i.e., α - and threshold-MAML).

A.4 Multi-dimensional regression on real data sets

In this section, we provide details on how the data sets used for multi-dimensional linear regression in the main document were divided into separate source and target tasks. We also visualize the inferred α weight values that are used for the predictions reported in Table 2, where the α -weighted methods provide a small improvement in RMSE over the uniformly-weighted methods.

Diabetes data. We split the diabetes data set into multiple sources by grouping on the following age groups: [19, 29), [29, 39), [39, 49), [53, 59), [59, 64), [64, 79). The target age group included data from the age group [49, 52].

Figure 7 (left) shows a visualization of the sources that were upweighted (blue) and downweighted (gray). In particular, the sources from the age groups [39, 49) and [64, 79) were upweighted, and the source corresponding to the age group of [19, 29) received 0 weight, which indicates that the closer age groups, i.e. [39, 49) and [64, 79), are more similar sources to learn from the younger age group [19, 29) for the target task (i.e., the age group [49, 52]).

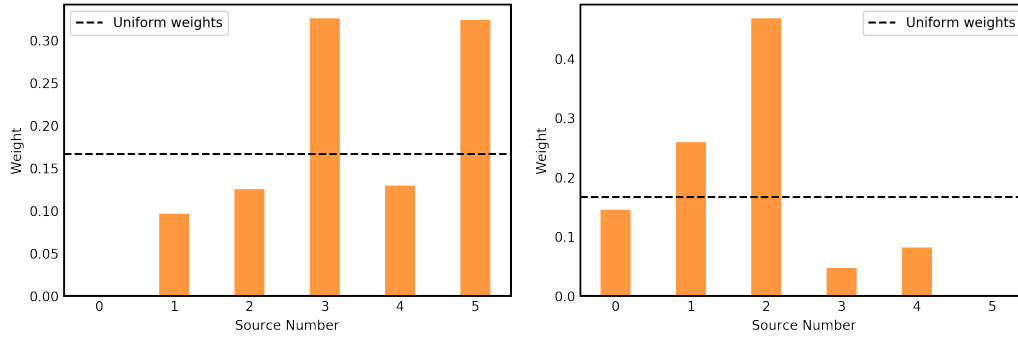


Figure 7: The learned α -weighting according to the kernel IPM between the α -mixture of sources and target. **Left:** Diabetes data set. **Right:** Boston data set.

Boston housing prices. The Boston housing prices data set was split into the sources by grouping the sources tasks on the following age groups: $[2.9, 29.1)$, $[29.1, 42.3)$, $[42.3, 58.1)$, $[72.5, 84.4)$, $[84.4, 92.4)$, and $[92.4, 100.0)$. The target age group included data from the age group $[58.1, 72.5)$.

The inferred α weight values are displayed in Figure 7 (right). Here we see that the sources corresponding to the age groups $[29.1, 42.3)$ and $[42.3, 58.1)$ are upweighted, while the source corresponding to the age group $[92.4, 100.0)$ received 0 weight.

References

- A. Achille, M. Lam, R. Tewari, A. Ravichandran, S. Maji, C. C. Fowlkes, S. Soatto, and P. Perona. Task2vec: Task embedding for meta-learning. In *ICCV*, pages 6430–6439, 2019.
- B. Adlam, C. Cortes, M. Mohri, and N. Zhang. Learning GANs and ensembles using discrepancy. In *NeurIPS*, pages 5788–5799, 2019.
- H. Altae-Tran, B. Ramsundar, A. S. Pappu, and V. Pande. Low data drug discovery with one-shot learning. *ACS central science*, 3(4):283–293, 2017.
- A. Antoniou, H. Edwards, and A. Storkey. How to train your maml. *arXiv e-print 1810.09502*, 2018.
- P. L. Bartlett and S. Mendelson. Rademacher and Gaussian complexities: Risk bounds and structural results. *JMLR*, pages 463–482, 2002.
- S. Ben-David, J. Blitzer, K. Crammer, A. Kulesza, F. Pereira, and J. W. Vaughan. A theory of learning from different domains. *Machine learning*, 79:151–175, 2010.
- C. Cortes and M. Mohri. Domain adaptation and sample bias correction theory and algorithm for regression. *Theoretical Computer Science*, 519:103–126, 2014.
- B. Efron, T. Hastie, I. Johnstone, R. Tibshirani, et al. Least angle regression. *The Annals of Statistics*, 32(2):407–499, 2004.
- A. Fallah, A. Mokhtari, and A. Ozdaglar. On the convergence theory of gradient-based model-agnostic meta-learning algorithms. *arXiv e-print 1908.10400*, 2019.
- C. Finn, P. Abbeel, and S. Levine. Model-agnostic meta-learning for fast adaptation of deep networks. In *ICML*, pages 1126–1135, 2017.
- C. Finn, K. Xu, and S. Levine. Probabilistic model-agnostic meta-learning. In *NeurIPS*, pages 9516–9527, 2018.
- C. Finn, A. Rajeswaran, S. Kakade, and S. Levine. Online meta-learning. In *ICML*, pages 1920–1930, 2019.
- E. Grant, C. Finn, S. Levine, T. Darrell, and T. Griffiths. Recasting gradient-based meta-learning as hierarchical Bayes. In *ICLR*, 2018.

- D. Harrison Jr and D. L. Rubinfeld. Hedonic housing prices and the demand for clean air. 1978.
- G. Jerfel, E. Grant, T. Griffiths, and K. A. Heller. Reconciling meta-learning and continual learning with online mixtures of tasks. In *NeurIPS*, pages 9119–9130, 2019.
- H. S. Jomaa, J. Grabocka, and L. Schmidt-Thieme. Dataset2vec: Learning dataset meta-features. *arXiv e-print 1905.11063*, 2019.
- M. Khodak, M.-F. Balcan, and A. Talwalkar. Provable guarantees for gradient-based meta-learning. In *ICML*, 2019a.
- M. Khodak, M.-F. F. Balcan, and A. S. Talwalkar. Adaptive gradient-based meta-learning methods. In *NeurIPS*, pages 5915–5926, 2019b.
- G. Koch. Siamese neural networks for one-shot image recognition. 2015.
- B. M. Lake, R. Salakhutdinov, and J. B. Tenenbaum. Human-level concept learning through probabilistic program induction. *Science*, 350(6266):1332–1338, 2015.
- Z. Li, F. Zhou, F. Chen, and H. Li. Meta-SGD: Learning to learn quickly for few-shot learning. *arXiv e-print 1707.09835*, 2017.
- Y. Mansour, M. Mohri, and A. Rostamizadeh. Domain adaptation: Learning bounds and algorithms. *arXiv e-print 0902.3430*, 2009a.
- Y. Mansour, M. Mohri, and A. Rostamizadeh. Domain adaptation with multiple sources. In *NeurIPS*, pages 1041–1048, 2009b.
- A. Müller. Integral probability metrics and their generating classes of functions. *Advances in Applied Probability*, 29(2):429–443, 1997.
- T. Munkhdalai and H. Yu. Meta networks. In *ICML*, pages 2554–2563, 2017.
- A. Nagabandi, C. Finn, and S. Levine. Deep online learning via meta-learning: Continual adaptation for model-based rl. *arXiv e-print 1812.07671*, 2018.
- A. Nichol, J. Achiam, and J. Schulman. On first-order meta-learning algorithms. *arXiv e-print 1803.02999*, 2018.
- B. Oreshkin, P. R. López, and A. Lacoste. Tadam: Task dependent adaptive metric for improved few-shot learning. In *NeurIPS*, pages 721–731, 2018.
- A. Pentina, E. SDSC, and C. H. Lampert. Multi-source domain adaptation with guarantees. In *NeurIPS 2019 Workshop on Machine Learning with Guarantees*, 2019.
- A. Rahimi and B. Recht. Random features for large-scale kernel machines. In *NeurIPS*, pages 1177–1184, 2008.
- S. Ravi and A. Beaton. Amortized Bayesian meta-learning. In *ICLR*, 2019.
- S. Ravi and H. Larochelle. Optimization as a model for few-shot learning. In *ICLR*, 2016.
- A. Santoro, S. Bartunov, M. Botvinick, D. Wierstra, and T. Lillicrap. Meta-learning with memory-augmented neural networks. In *ICML*, pages 1842–1850, 2016.
- C. Shui, M. Abbasi, L.-É. Robitaille, B. Wang, and C. Gagné. A principled approach for learning task similarity in multitask learning. *arXiv e-print 1903.09109*, 2019.
- J. Snell, K. Swersky, and R. Zemel. Prototypical networks for few-shot learning. In *NeurIPS*, pages 4077–4087, 2017.
- X. Song, W. Gao, Y. Yang, K. Choromanski, A. Pacchiano, and Y. Tang. ES-MAML: Simple Hessian-free meta learning. In *ICLR*, 2020.
- B. K. Sriperumbudur, K. Fukumizu, A. Gretton, B. Schölkopf, G. R. Lanckriet, et al. On the empirical estimation of integral probability metrics. *Electronic Journal of Statistics*, 6:1550–1599, 2012.

- S. C. Tan and J. P. San Lau. Time series clustering: A superior alternative for market basket analysis. In *Proceedings of the First International Conference on Advanced Data and Information Engineering (DaEng-2013)*, pages 241–248. Springer, Singapore, 2014.
- M. Vartak, A. Thiagarajan, C. Miranda, J. Bratman, and H. Larochelle. A meta-learning perspective on cold-start recommendations for items. In *NeurIPS*, pages 6904–6914, 2017.
- O. Vinyals, C. Blundell, T. Lillicrap, D. Wierstra, et al. Matching networks for one shot learning. In *NeurIPS*, pages 3630–3638, 2016.
- R. Vuorio, S.-H. Sun, H. Hu, and J. J. Lim. Toward multimodal model-agnostic meta-learning. *arXiv e-print 1812.07172*, 2018.
- Z. Xu, L. Cao, and X. Chen. Meta-learning via weighted gradient update. *IEEE Access*, 7:110846–110855, 2019.
- H. Yao, Y. Wei, J. Huang, and Z. Li. Hierarchically structured meta-learning. *arXiv e-print 1905.05301*, 2019.
- J. Yoon, T. Kim, O. Dia, S. Kim, Y. Bengio, and S. Ahn. Bayesian model-agnostic meta-learning. In *NeurIPS*, pages 7332–7342, 2018.
- C. Zhang, L. Zhang, and J. Ye. Generalization bounds for domain adaptation. In *NeurIPS*, pages 3320–3328, 2012.
- C. Zhang, L. Zhang, and J. Ye. Generalization bounds for domain adaptation. *arXiv e-print 1304.1574*, 2013.
- P. Zhang, Q. Liu, D. Zhou, T. Xu, and X. He. On the discrimination-generalization tradeoff in GANs, 2018.
- X. S. Zhang, F. Tang, H. H. Dodge, J. Zhou, and F. Wang. Metapred: Meta-learning for clinical risk prediction with limited patient electronic health records. In *KDD*, pages 2487–2495, 2019.